Available online at www.sciencedirect.com
SCIENCE DIRECT
Surface Science 600 (2006) 1048–1053
SURFACE SCIENCE
www.elsevier.com/locate/susc

Study of $c(2\times2)$-MnAu(001) layers on Mn(001) by means of scanning tunneling microscopy/spectroscopy

T.K. Yamada [a,*], A.L. Vázquez de Parga [b], M.M.J. Bischoff [c], T. Mizoguchi [a], H. van Kempen [c]

[a] Department of Physics, Faculty of Science, Gakushuin University, 1-5-1 Mejiro, 171-8588 Toshima, Tokyo, Japan
[b] Departamento de Fisica de la Materia Condensada e Instituto de Ciencia de Materiales "Nicolas Cabrera", Universidad Autónoma de Madrid, Cantoblanco 28049, Madrid, Spain
[c] Institute for Molecules and Materials, Radboud University Nijmegen, Toernooiveld 1, 6525 ED Nijmegen, The Netherlands

Received 15 October 2005; accepted for publication 19 December 2005
Available online 19 January 2006

Abstract

Intermixing, growth, geometric and electronic structures of gold films grown on antiferromagnetic stacking body-centered-tetragonal manganese (001) films were studied by means of scanning tunneling microscopy/spectroscopy at room temperature in ultra-high vacuum. We found stable ordered $c(2\times2)$-MnAu(001) alloy layers after depositing Au on pure Mn layers. Since at the fourth layer (5×23)-like Au reconstruction appears instead of the $c(2\times2)$ structure and local density of states peaks obtained on the $c(2\times2)$-MnAu surface disappear, pure Au layers likely grow from the fourth layer.

Keywords: Scanning tunneling microscopy; Scanning tunneling spectroscopies; Surface structure, morphology, roughness, and topography; Metallic films; Gold; Manganese; Alloys; Metal–metal interfaces

1. Introduction

To prevent oxidization of magnetic films a gold coating has been widely used. However, it is difficult to grow a pure gold atomic layer on magnetic films. Au on Fe(001) was a good candidate because Fe and Au are immiscible in bulk, Fe has a much higher surface energy than Au, and the lattice mismatch between Fe(001) and Au(001) is only 0.5%. Despite of these favourable circumstances it was found that an FeAu surface alloy layer forms with a $c(2\times2)$ structure [1].

There have been many studies of magnetic films grown on noble metals [2], but much less studies of noble films on magnetic surfaces. Due to the large difference in surface energy, the substrate noble metal prefers to segregate on top of the magnetic films during the growth. Manganese has lower surface energy than noble metals. (Surface energies are 1.333 J/m^2 for Au, 1.298 J/m^2 for Mn, and 2.123 J/m^2 for Fe [3].) Several studies of Mn films grown on noble metal substrates: Au(001) [4], Ag(001) [5], and Cu(001) [6–18] have been reported. One monolayer Mn grown on Cu(001) forms MnCu alloy layers with a $c(2\times2)$ ordered structure. Mn atoms in the $c(2\times2)$ structure have a high local magnetic moment, a ferromagnetic in-plane order, and an antiferromagnetic coupling between layers [13]. A $c(2\times2)$ alloy layer is also observed for Mn/Au(001) and Mn/Ag(001). However, for the Au(001) substrate, a pure Au layer or a pure Mn layer is also formed depending on different annealing processes [4], i.e., it is difficult to grow an well ordered $c(2\times2)$ alloy structure only.

In this study we show the first study of growth, intermixing, and geometric structure of Au films grown on an ordered antiferromagnetic stacking body-centered-tetragonal Mn(001) film by means of scanning tunneling

* Corresponding author. Tel.: +81 3 3986 0221; fax: +81 3 5992 9319.
E-mail addresses: 20030303@gakushuin.ac.jp (T.K. Yamada), H.vanKempen@science.ru.nl (H. van Kempen).

0039-6028/$ - see front matter © 2006 Elsevier B.V. All rights reserved.
doi:10.1016/j.susc.2005.12.027

microscopy (STM)/spectroscopy (STS) at room temperature (RT) in ultra-high vacuum (UHV). STM/STS measurements show that, even at room temperature, stable $c(2\times2)$-MnAu(001) alloy layers are formed. Since on the fourth layer STM images show (5×23)-like Au reconstruction and STS data show an absence of local density of states peaks observed on the $c(2\times2)$-MnAu(001) alloy surface, we conclude that pure Au layers grow from the fourth layer.

2. Experimental details

STM and STS measurements were performed in UHV ($\sim5\times10^{-11}$ mbar) at RT with a commercial STM.

In this study, we used W tips prepared as follows: in air, a W polycrystalline wire (purity 99.99%) with a diameter of 0.5 mm was chemically etched with 5 M KOH aq. and subsequently, it was moved into UHV (1×10^{-10} mbar). Then, the tip was sputtered by Ar^+ and heated by electron-bombardment.

An Fe(001) whisker was used as a substrate. This Fe(001) whisker was cleaned by sputtering and annealing cycles. After this cleaning process, less than 1% oxygen contaminants were measured by Auger spectroscopy and atomically and chemically resolved STM images [19–21]. About 7 ML of Mn (purity 99.999%) was grown on the Fe(001) whisker at 370 K at a pressure below 4×10^{-10} mbar. There is no intermixing of Fe into Mn layers above the third Mn layer [21]. Mn layers grown on Fe(001) have a body-centered tetragonal (bct) structure with the same in-plane lattice constant as Fe(001): 0.287 nm and an interlayer distance of 0.165 nm [21]. Au films were deposited on the bct Mn(001) layers at RT with a rate of 0.25 ML/min at a pressure below 3×10^{-10} mbar. The Au thickness is determined by calibrating the evaporation rate with the atomically and chemically resolved STM images and the values given by the quartz balance.

Spectroscopy measurements were performed in the following way: $I(V)$ curves were obtained at every pixel of a constant current topographic image by opening the STM feedback loop at a given current and voltage (set point). dI/dV curves were obtained by numerical differentiation of the $I(V)$ curves.

3. Results and discussion

Fig. 1(a) shows an atomically resolved STM image obtained on the surface after deposition of 7 ML of Mn at 370 K on the Fe(001)-whisker. On the Mn(001) surface, usually, we observed only $p(1\times1)$-Mn(001) atoms and oxygen contaminants at the fourfold hollow sites (<1% concentration). However, the surface of a 1 ML Au layer grown on the Mn(001) film shows a different structure (Fig. 1(b)). By comparing Fig. 1(a) and (b) we conclude that the first Au layer forms a $c(2\times2)$ structure. Our Auger spectra show a Mn 40 eV peak and a Au 69 eV peak. No Fe 47 eV peak was observed, from which we estimate that the Fe concentration is below 4%. (The half width of the Auger peak is 1.5 eV.)

Thus, the $c(2\times2)$ structure consists of only Au and Mn. Since Au and Mn are miscible and similar $c(2\times2)$ alloy layers are also found on Mn films grown on noble metal(001) [4–18], the observed $c(2\times2)$ structure is considered to be a $Mn_{50}Au_{50}$ alloy. Fig. 1(c) shows a model of the $p(1\times1)$-Mn(001) structure and the $c(2\times2)$-MnAu(001) alloy structure. Since Au has a larger atomic size, Au atoms might buckle from the surface and appear brighter in Fig. 1(b). However, this speculation might be wrong since a study of MnCu-$c(2\times2)$-surface-alloy showed that Mn appears brighter in STM images due to a strong electronic effect [18].

Fig. 2 shows STM images obtained on the surface of a 0.4 ML (a), a 0.7 ML (b), and a 2.2 ML (c) Au film grown on a 7 ML Mn(001) film. Due to a layer-plus-island growth mode, odd and even Mn layers are exposed as shown in Fig. 2(a). The Au layer grows in a layer-by-layer mode (Fig. 2(b)). The roughness of the surface increases with the coverage, but the films grow still epitaxially (Fig. 2(c)). In all the layers exposed on the surface, there are areas that are slightly brighter than the rest of the terrace. The distribution of these bright areas changes with the thickness: 19% for the first layer, 45% for the second

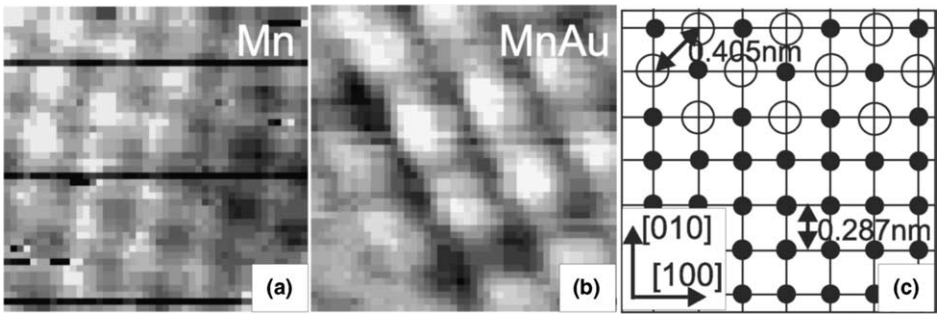

Fig. 1. (a) shows an atomically resolved STM image obtained on the surface of a 7 ML Mn film grown at 370 K on the Fe(001)-whisker (1.7×1.7 nm^2). A $p(1\times1)$-Mn(001) structure is observed. (b) shows an atomically resolved STM image obtained on the surface of a 1 ML Au film grown at RT on the Mn(001) film (1.7×1.7 nm^2). A $c(2\times2)$-MnAu alloy structure is observed. (c) A model of the atomic configurations. Dots and white-circles denote Mn and Au atoms, respectively. Lines denote the atomic lattice.

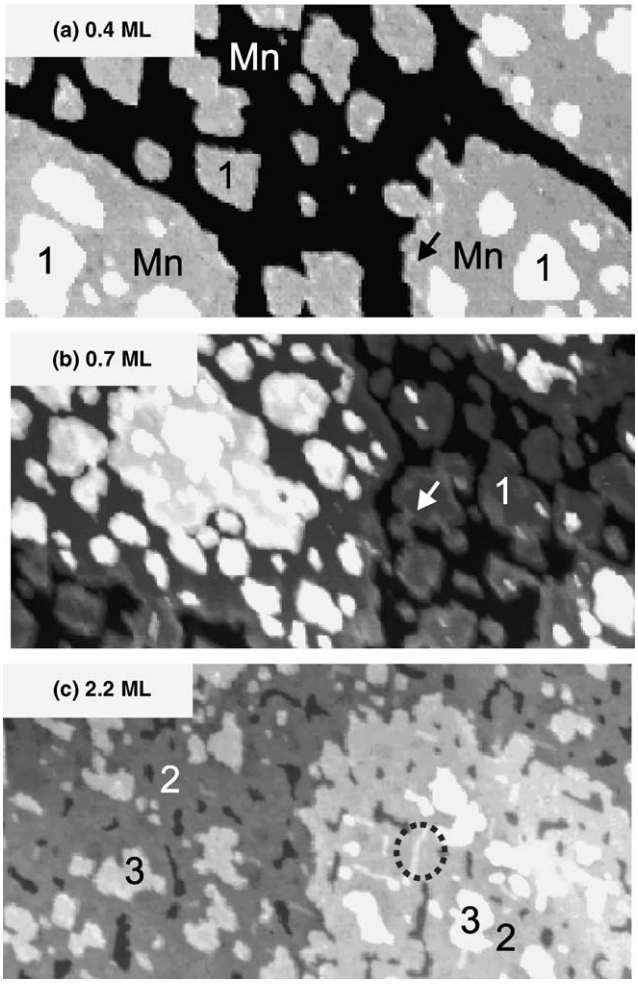

Fig. 2. STM topographic images obtained on the Mn surface covered by Au films with coverages of (a) 0.4 ML ($V_S = -1$ V, $I = 0.1$ nA), (b) 0.7 ML ($V_S = -0.5$ V, $I = 0.1$ nA), and (c) 2.2 ML ($V_S = +0.8$ V, $I = 0.1$ nA) (100×50 nm^2). Arrows and the dotted circle denote bright areas, which are 0.05 ± 0.01 nm higher than the surrounding terrace. Numbers denote the stacking numbers of the layers.

layer, and 43% for the third layer. On the first layer, these are observed around steps as marked by arrows in Fig. 2(a) and (b) and dotted circles in Fig. 3(a). On the second layer, these are observed in the middle of the terraces, e.g., as shown in the dotted-circle in Fig. 2(c). The height of these bright areas/lines is about 0.05 ± 0.01 nm with respect to the surrounding terrace. The origin of these bright areas/lines is discussed later.

Fig. 3(a) shows an atomically resolved STM image obtained on the Mn surface after deposition of 0.6 ML of Au at RT. The Mn terrace and the first Au layer show a $c(2 \times 2)$ structure. The observed structure in Fig. 3 is considered to be a $c(2 \times 2)$-MnAu surface alloy, i.e., now the top Mn layer (“0”) and the first Au layer (“1”) mix completely and form the $c(2 \times 2)$ structure.

Fig. 3(b) shows another atomically resolved STM image obtained on the surface of Mn films covered by a 1 ML Au film. Most terraces are the first layer (“1”) and the second layer is observed as islands (“2”). The original Mn surface

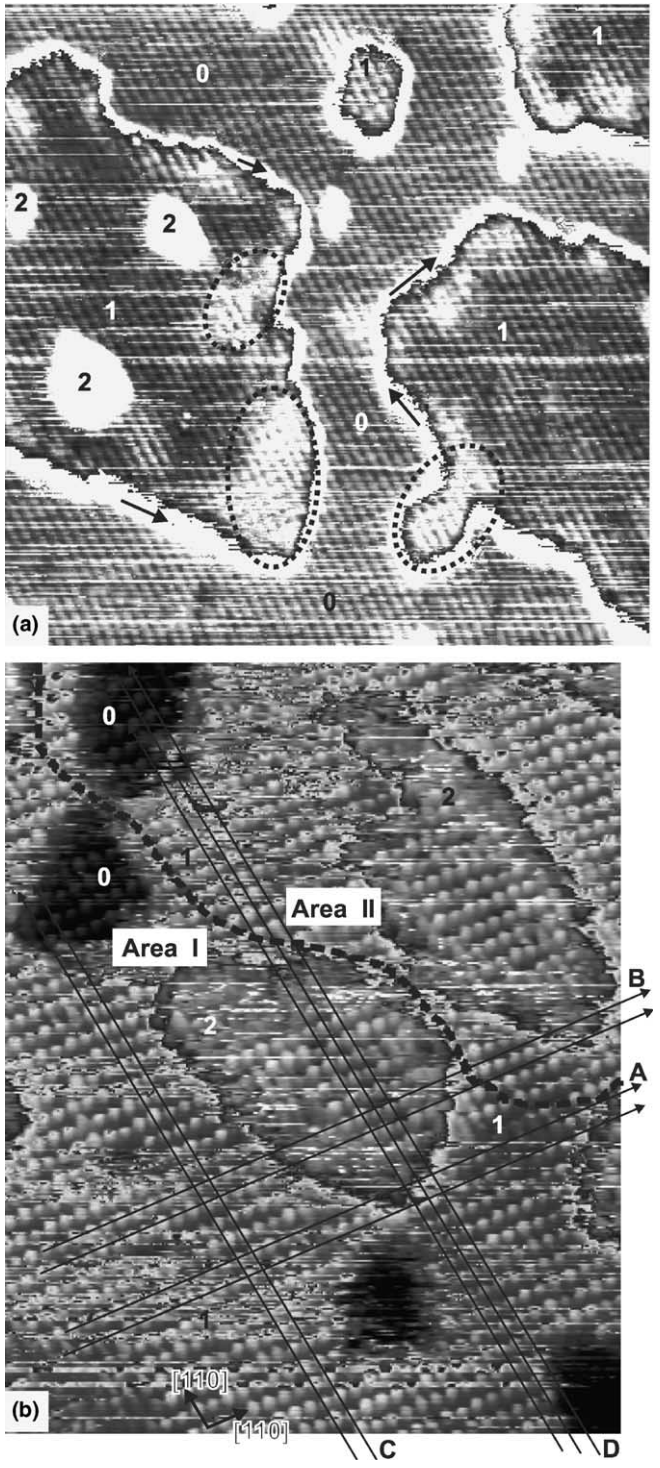

Fig. 3. (a) shows an atomically resolved STM image obtained on the Mn surface covered by a 0.6 ML Au film at RT (20×20 nm^2, $V_S = -14$ mV, $I = 3.3$ nA). The surface shows the $c(2 \times 2)$ structure of the MnAu surface alloy. Near the step edge, the first layer appears brighter (dashed circles). The white lines outside the islands marked by black arrows are an artifact of the jumped grey-scale. Numbers denote the stacking numbers of the layers. (b) shows an atomically resolved STM image obtained on the Mn surface covered by a 1 ML Au film at RT (16×13 nm^2, $V_S = -3$ mV, $I = 8.5$ nA). In (b) arrows: A–D are guides for the eye. Numbers denote the stacking numbers of the layers. The dashed line denotes a domain boundary. To make the atomic features more prominent, the contrast in (a and b) has been adjusted in every terrace.

is observed in depressions (“0”). All layers completely mix with Mn and form the $c(2\times2)$-MnAu(0 0 1) structure. It is found that there is a default line (a black dashed line in Fig. 3(b)). The lower and the upper sides of the default line are named “Area I” and “Area II”, respectively. The arrows marked “A, B” (“C, D”) follow the [1 1 0] ([1 $\bar{1}$ 0]) direction. Following the arrows “A” shows that the protrusions are on the arrows. On the other hand, following the arrows “B” from the area I to the area II shows that the arrows have to be slipped half a lattice constant along the [1 $\bar{1}$ 0] direction to keep on the protrusions. The same atomic configuration is also observed along the [1 $\bar{1}$ 0] direction. Although following the arrows “C, D” in the area I shows that the arrows are on the protrusions for the layers “0, 1, and 2”, following the arrows “D” from the area I to the area II shows that the arrows have to be slipped half a lattice constant along the [1 1 0] direction to keep on the protrusions. Thus, from the area I to the area II, protrusions shift half a lattice constant along both [1 1 0] and [1 $\bar{1}$ 0] directions. These domain walls are a straightforward result of the fact that two different $c(2\times2)$ lattices can be accommodated on the $p(1\times1)$ lattice, shifted with a $p(1\times1)$ period.

Fig. 4 was obtained on the Mn surface covered by a 2.2 ML Au film. The second (“2”) and the third (“3”) layers are observed as a terrace and islands, respectively. The second and the third layers show the $c(2\times2)$ structure, but islands that consist of less than 80 protrusions show a $p(1\times1)$ structure. Probably, this structure is formed by one single element, i.e., Au or Mn. If these are pure Au islands, these Au atoms have in-plane lattice constants similar to the substrate bct-Mn(0 0 1), which has the same in-plane lattice constant as the bcc-Fe(0 0 1), i.e., 0.287 nm. The height of the $p(1\times1)$ islands is the same as the height of the $c(2\times2)$ islands of the third layer. On the surface of the layer “2”, the presence of domain boundaries is very clear (dashed lines in Fig. 4).

Although the $c(2\times2)$ structure was observed up to the third layer, no clear ordered structure was observed on the fourth layer. Fig. 5(a) was obtained on the Mn surface covered by a 4.0 ML Au film at RT. The STM images show not only flat terraces, but also many bright areas (47%) on the fourth layer (Fig. 5(a)). Although this is comparable to the results obtained on the first three layers, the difference is that now the bright areas make periodic rows (Fig. 5(b)). The width of each row is about 1.5 nm (Fig. 5(c)). The corrugation of the rows is about 0.05 nm. These parallel arrangement and the width are similar to the (5×23) reconstruction of Au(0 0 1) [22]. The reconstruction is also present on Au layers deposited on Fe(0 0 1) [1]. The presence of these structures indicates that a pure Au layer starts from the fourth layer. It should be mentioned that the bright rows follow the [1 0 0] or the [0 1 0] direction.

The step heights (=interlayer distances) were measured from the STM images. First, we diminished the distortion in the STM image with a plane-fitting. Then, we made a histogram from this STM image. Each atomic layer appears as a sharp peak. By measuring the distance between the peaks, we obtained the step heights with an error of

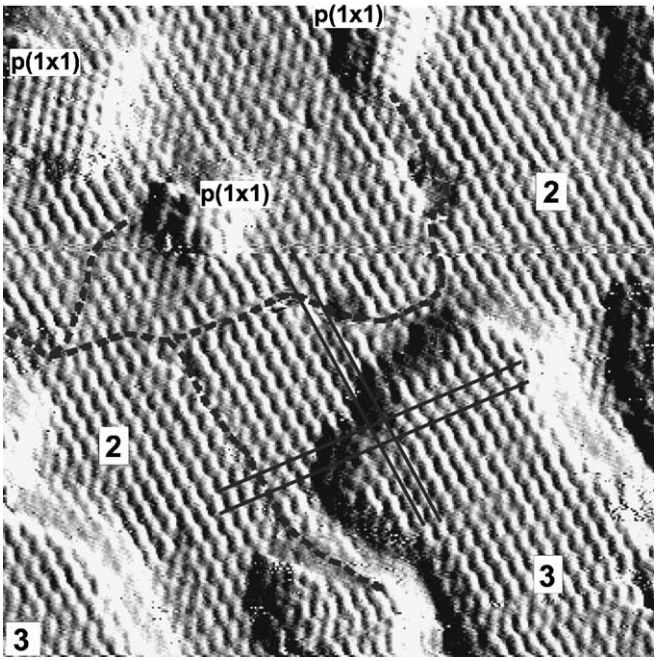

Fig. 4. This figure shows an atomically resolved STM image in constant current mode obtained on the Mn surface covered by a 2.2 ML Au film at RT (14×14 nm^2, $V_S=-12$ mV, $I=3$ nA). Numbers denote different heights on the image. Black lines are guides for the eye. Dashed lines denote domain boundaries. To make the atomic features more prominent, the derivative of the constant current image is shown.

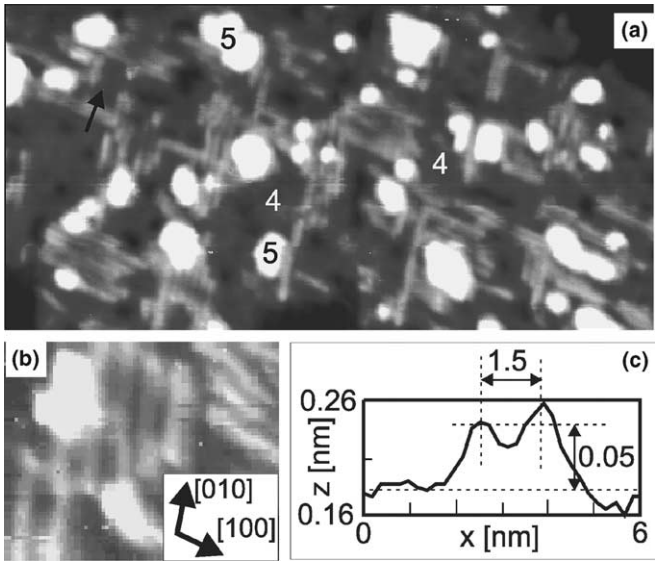

Fig. 5. (a) shows an STM image obtained on the Mn surface covered by a 4.0 ML Au film at RT (100×50 nm^2, $V_S=-0.5$ V, $I=0.5$ nA). Numbers in (a) denote the stacking numbers of the layers. (b) shows an enlarged image from (a) (14×11 nm^2). Periodic rows are observed, which follow the [1 0 0] or the [0 1 0] direction. (c) shows a line profile along the black arrow in (a). The periodic rows have a corrugation of ~0.05 nm. The width of a bright row is about 1.5 nm.

±0.007 nm. The error was obtained from the half width at half maximum of the peak.

The obtained apparent step heights are influenced by the electronic structure of the sample surface (the sample local density of states (LDOS) as well as the barrier heights). To check the influence of the sample LDOS, the apparent step heights were measured as a function of the sample bias voltage. Barrier height measurements were not performed. (All measurements shown in Fig. 6 were obtained between the $c(2\times2)$-alloy layers. It is assumed that all $c(2\times2)$-alloy layers have the same work function.) Fig. 6 shows the apparent step heights as a function of the sample bias voltage. h_{ij} denotes the step height between the layer i and j. Since the STM images obtained at the voltage set point above the Fermi energy include influences of the sample LDOS, the step heights obtained at high negative voltages (<1 V) are believed to show the real geometric step heights. The interlayer distances obtained are 0.168 ± 0.007 nm for h_{01}, 0.170 ± 0.007 nm for h_{12}, and 0.170 ± 0.007 nm for h_{23}. This is a little larger than the interlayer distance of the bct-Mn(001) (0.165 nm).

From all these STM images we propose a possible model for each Au coverage (Fig. 7). Since the Au and Mn are miscible in the bulk, dealloying as in the case of Au on Fe is unlikely [1]. So, after deposition of 3 ML of Au the surface layer is still a $c(2\times2)$ MnAu alloy, and we speculate that the layers underneath are also alloyed layers. On the MnAu-alloy layers bright areas were always observed with a height of 0.05 ± 0.01 nm. This height was also checked to be independent of the sample bias voltage (Figs. 2–5 were obtained at several voltages between −1.2 and +0.8 V). Thus, we believe that this height difference is not due to an electronic effect, but to a change in geometric structure. After deposition of 4 ML of Au, six layers of MnAu-$c(2\times2)$-alloy are formed and an additional layer is formed on the top. If the bright rows of the top layer are an indication of Au (5×23) reconstruction [22], we speculate that the layers on the MnAu-alloy-layers consist of pure Au. The experimentally obtained interlayer distances are 0.165 nm for Mn(001), 0.170 nm for the MnAu-alloy, and 0.220 nm for the bright rows on the Au layers.

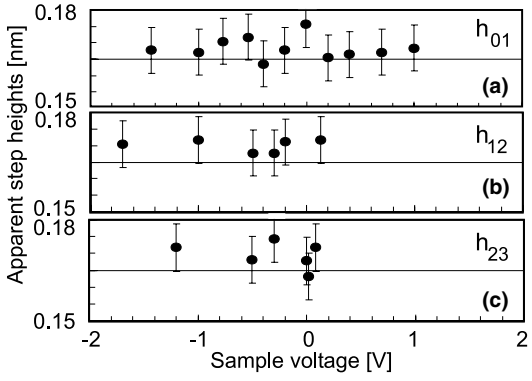

Fig. 6. Apparent step heights of the films of the Au/Mn(001) layers. h_{ij} denotes the step height between the layer i and j. The step heights were obtained by measuring the distance between the sharp peaks in the histogram.

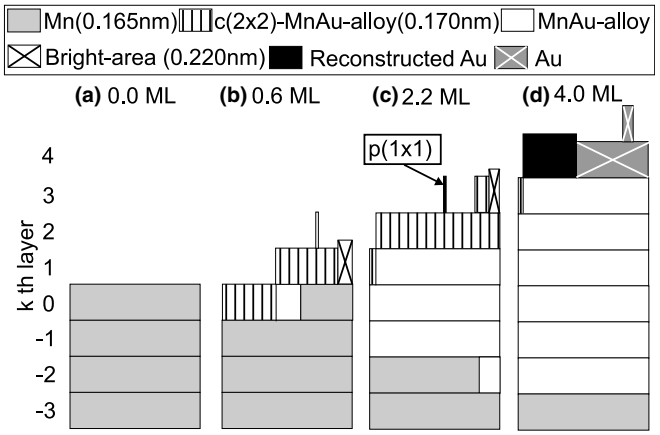

Fig. 7. Models of the Mn films covered by Au films of (a) 0 ML, (b) 0.6 ML, (c) 2.2 ML and (d) 4.0 ML. (b)–(d) correspond to Figs. 3–5, respectively.

At the bright areas on the MnAu-alloy layers, atomically resolved images showed the $c(2\times2)$ structure, i.e., no difference in the in-plane lattice constant, and only the interlayer distance expands 0.05 ± 0.01 nm. These bright areas were observed near steps. The atoms at steps have lower coordination and therefore they can relax the strain easily, so the bright areas are probably caused by the relaxation of strain. In bulk, it is known that MnAu alloy has a bct (CsCl-type) structure with an in-plane (out-of-plane) lattice constant of 0.318 nm (0.328 nm) [23]. Since the in-plane lattice constant of the observed MnAu(001)-alloy is 0.405 nm, the large difference in the in-plane lattice constant might be a cause of the strain.

By taking spectroscopy curves LDOS on the sample surface were studied. In our previous study LDOS peaks of the $c(2\times2)$-MnAu(001) were found at +0.1 V, +0.9 V, and +1.9 V above the Fermi energy in dI/dV curves, which were normalized by the tunneling probability function [24]. The atomically resolved images show that pure Au layers likely grow from the fourth layer. To confirm this statement LDOS of the fourth and the fifth layers were studied. Fig. 8 was obtained on the Mn surface coated by a 4 ML Au film. The STM image shows the fourth and the fifth layers (Fig. 8(a)). The dI/dV curves obtained on the fourth ("4") and the fifth ("5") layers are the same, but the dI/dV curves do not show any peaks or shoulders above the Fermi energy (Fig. 8(b)). Also, dI/dV curves obtained from the reconstructed areas ("R" in Fig. 8(a)) show no peaks. The normalized $(dI/dV)/T$ curves represent the sample LDOS [21,24]. $(dI/dV)/T$ curves in Fig. 8(b) show that the fourth and the fifth layers do not have any LDOS peaks, i.e., the fourth and the fifth layers have a different crystalline structure or composition compared to the $c(2\times2)$ MnAu layer. The difference in the dI/dV curves obtained on the fourth layer and the reconstructed areas is probably caused by a different work function on the recon-

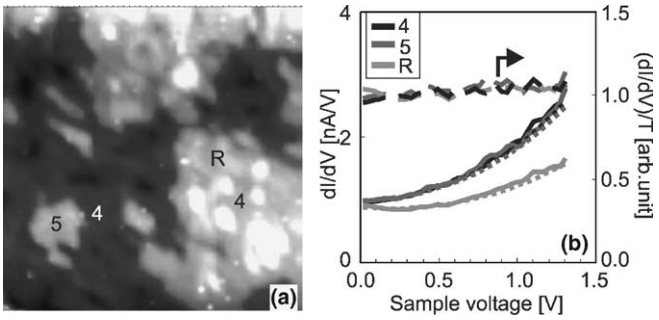

Fig. 8. (a) shows an STM image obtained with a W tip on the Mn surface covered by a 4 ML Au film at RT (54×55 nm^2, $V_S = -0.5$ V, $I = 0.5$ nA). Numbers denote the stacking numbers of the layers. "R" denotes the bright-row areas (cf. Fig. 5). (b) shows dI/dV curves (solid lines), fits of the tunneling probability function to the dI/dV curves (dotted lines), and (dI/dV)/T curves (dashed lines). Black, dark grey, and bright grey curves were obtained from "4", "5", and "R" in (a), respectively.

structed areas since LDOS are featureless for both areas. The change in work function could be related to a change in composition, i.e., the reconstruction areas include no intermixed Mn atoms.

4. Conclusion

Intermixing, growth, geometric and electronic structures of gold films grown on antiferromagnetic stacking body-centered-tetragonal manganese (001) films were studied by means of scanning tunneling microscopy/spectroscopy at room temperature in ultra-high vacuum. We found stable ordered $c(2 \times 2)$-MnAu(001) alloy layers after depositing Au on pure Mn films. The alloy layers have an in-plane (an out-of-plane) lattice constant of 0.405 nm (0.340 nm). From the fourth layer on, no $c(2 \times 2)$ alloy structure is observed and a (5×23)-like Au reconstruction is seen. Also, LDOS peaks of the $c(2 \times 2)$-MnAu surface disappear from the fourth layer. These observations indicate that pure Au layers start to grow from the fourth layer.

Acknowledgments

This work was supported by the Stichting voor Fundamenteel Onderzoek der Materie (FOM), which is funded by the Nederlandse Organisatie voor Wetenschappelijk Onderzoek (NWO), and the European Growth Project MAGNETUDE. We are especially grateful to D.T. Pierce for supplying us with the Fe whiskers. A.L.V.P. acknowledges the financial support by the Ministerio de Educacion y Ciencia (MEC) through Project No. FIS2004-01026. T.K.Y. acknowledges Grant-in-Aid for JSPS Fellows. H.v.K. acknowledges a DVF from the International Research Center for Experimental Physics (IRCEP) at the Queen's University, Belfast (Ireland) and Instituto Universitario de Ciencia de Materials "Nicolas Cabrera" at the Universidad Autónoma de Madrid (Spain).

References

[1] M.M.J. Bischoff, T. Yamada, A.J. Quinn, R.G.P. van der Kraan, H. van Kempen, Phys. Rev. Lett. 87 (2001) 246102.
[2] F.J. Himpsel, J.E. Ortega, G.J. Mankey, R.F. Willis, Adv. Phys. 47 (1998) 511.
[3] W.R. Tyson, W.A. Miller, Surf. Sci. 62 (1977) 267.
[4] W. Kim, S.-J. Oh, J. Seo, H.G. Min, S.C. Hong, J.-S. Kim, Phys. Rev. B 65 (2002) 205407.
[5] P. Schieffer, C. Krembel, M.-C. Hanf, G. Gewinner, Y. Gauthier, Phys. Rev. B 65 (2002) 235427.
[6] M. Wuttig, Y. Gauthier, S. Blügel, Phys. Rev. Lett. 70 (1993) 3619.
[7] H.P. Noh, T. Hashizume, D. Jeon, Y. Kuk, H.W. Pickering, T. Sakurai, Phys. Rev. B 50 (1994) 2735.
[8] R.G.P. van der Kraan, H. van Kempen, Surf. Sci. 338 (1995) 19.
[9] O. Rader, W. Gudat, C. Carbone, E. Vescovo, S. Blügel, R. Kläsges, W. Eberhardt, M. Wuttig, J. Redinger, F.J. Himpsel, Phys. Rev. B 55 (1997) 5404.
[10] T. Flores, S. Junghans, M. Wuttig, Surf. Sci. 371 (1997) 14.
[11] D. Brown, T.C.Q. Noakes, D.P. Woodruff, P. Bailey, Y.Le. Goaziou, J. Phys. Condens. Matter 11 (1999) 1889.
[12] D. Wortmann, S. Heintz, G. Bihlmayer, S. Blügel, Phys. Rev. B 62 (2000) 2862.
[13] M. Eder, J. Hafner, E.G. Moroni, Phys. Rev. B 61 (2000) 11492.
[14] Y. Huttel, S. Gallego, M.C. Muñoz, M.C. Asensio, Surf. Sci. 482–485 (2001) 540.
[15] F. Schiller, S. Danzenbacher, C. Laubschat, Surf. Sci. 482–485 (2001) 442.
[16] S. Gallego, F. Sonia, M.C. Muñoz, Surf. Sci. 524 (2003) 164.
[17] T. Bernhard, R. Pfandzelter, H. Winter, Surf. Sci. 543 (2003) 36.
[18] D. Wortmann, S. Heinze, G. Bihlmayer, S. Blügel, Phys. Rev. B 62 (2000) 2862.
[19] F. Besenbacher, E. Laegsgaard, L.P. Nielsen, L.R. Ruan, I. Stensgaard, J. Vac. Technol. B 12 (1994) 1758.
[20] E.L.D. Hebensteit, W. Hebenstreit, M. Schmid, P. Varga, Surf. Sci. 441 (1999) 441.
[21] T.K. Yamada, M.M.J. Bischoff, T. Mizoguchi, H. van Kempen, Surf. Sci. 516 (2002) 179.
[22] O.S. Hernan, A.L. Vázquez de Parga, J.M. Gallego, R. Miranda, Surf. Sci. 415 (1998) 106.
[23] S. Chikazumi, K. Ohta, K. Adachi, N. Tsuya, Y. Ishikawa (Eds.), Handbook of Magnetic Material, Asakura-Shoten Co., 1975.
[24] T.K. Yamada, R. Robles, E. Martinez, M.M.J. Bischoff, A. Vega, A.L. Vázquez de Parga, T. Mizoguchi, H. van Kempen, Phys. Rev. B 72 (2005) 014410.